Elastic anisotropic full waveform inversion using probabilistic petrophysical constraints

Odette Aragao & Paul Sava

Center for Wave Phenomena and Dept. of Geophysics, Colorado School of Mines, Golden CO 80401
aquinodearagao@mines.edu

ABSTRACT

Full waveform inversion (FWI) is formulated as an inverse problem driven by a wave equation and it works by iteratively minimizing an objective function that measures the misfit between observed and predicted data in the least-squares sense. However, FWI suffers from significant problems. First, the objective function is multimodal and thus the inverse problem solved by gradient techniques may not lead to the globally optimal solution. This phenomenon is due to cycle skipping which occurs when the starting models are unable to predict data that match the observed data to better than half a cycle at the lowest usable frequencies available within the data set. Second, as the simulated data are computed using a two-way wave equation, all wave propagation mechanisms are not adequately considered if one does not assume a structure of the stiffness tensor that truly represents the subsurface. Third, FWI implementations using an elastic wave equation estimate multiple parameters representing different physical properties of the subsurface, which increases the null space of the parameter space, leading to a larger domain of ambiguity and increasing the number of models that can equally well explain the data. Depending on the parameterization used for inversion, elastic properties may be coupled and updates of one parameter may impact others, an effect known as interparameter crosstalk. In addition, some combinations of model parameters can be lithologically implausible or impossible (e.g., negative Poisson ratio), and thus not represent feasible lithological units. We derive anisotropic models of subsurface properties using elastic full-waveform inversion and explicitly impose petrophysical penalties to guide models toward realistic lithology, i.e., to models consistent with the seismic data as well as with the petrophysical context in the area of study. This methodology reduces the potential negative impact of cycle skipping, mitigates the artifacts created by interparameter crosstalk, and avoids geologically implausible earth models. We define this penalty using probability density functions (PDFs) derived from petrophysical information, such as well logs. The combined FWI objective function leads to robust anisotropic subsurface models that represent plausible lithologies, while at the same time leading to data predictions consistent with the observations.

Key words: full-waveform inversion, elastic, anisotropic, petrophysics

1 INTRODUCTION

Full waveform inversion (FWI) relies on accurate wavefield simulation, and thus seismic modeling should simulate the physics of wave propagation as accurately as possible. A common assumption in conventional FWI is that the subsurface is described by isotropic model parameters. Compared to implementations using the isotropic acoustic wave equation (Tarantola, 1984; Pratt et al., 1996), elastic FWI more accurately describes the physics of wave propagation in the subsurface (Tarantola, 1988), for example by representing correctly the amplitude behavior of seismic waves, as well as mode conversions. However, the increasing number of acquired offsets and azimuths require that we also account for the influence of anisotropy as an indispensable factor in fitting seismic field data (Plessix and Cao, 2010). Seismic anisotropy is particularly important to account for the different scales

of subsurface heterogeneity, within the signal bandwidth, as well as alignment of subsurface cracks and layers (Tsvankin, 2012). However, the intrinsic non-linearity, ill-posedness, and interparameter trade-off of elastic anisotropic FWI increases the possibility of being trapped in local minima and the likelihood of generating geologically infeasible inverted models (Operto et al., 2013).

A natural fix for this problem is to explicitly incorporate petrophysical information into elastic full waveform inversion and constrain wavefield inversion to models that satisfy prior knowledge about the subsurface model properties, and their petrophysical relationships. Aragao and Sava (2020a,b) explicitly incorporate petrophysical information in elastic FWI to recover models that honor both geophysical and petrophysical data. They achieve this goal by incorporating a penalty function, based on a single probability density function (PDF) (Aragao and Sava, 2020a) or on multiple PDFs (Aragao and Sava, 2020b), into the elastic isotropic FWI objective function. In order to recover anisotropic models, we use a petrophysical penalty similar to the one proposed by Aragao and Sava (2020a,b) to guide multidimensional anisotropic models towards solutions that satisfy the known anisotropic petrophysical properties.

2 METHOD

Consider the elastic wave equation,

$$\rho \frac{\partial^2 u_i}{\partial t^2} = \frac{\partial}{\partial x_j}\left(c_{ijkl}\frac{\partial u_l}{\partial x_k}\right) + f_i, \tag{1}$$

where $\mathbf{u}(e,\mathbf{x},t)$ is the elastic displacement, $\mathbf{f}(e,\mathbf{x},t)$ is the source function, e, $\mathbf{x}$ and t are, respectively, the experiment index, space coordinates and time, and $\underline{\underline{\mathbf{c}}}$ is the stiffness tensor.

The stiffness matrix C for a VTI media has 5 different coefficients: C_{11}, C_{13}, C_{33}, C_{55} and C_{66}. These elements, combined with density ρ, are used to determine the Thomsen parameters:

- P-wave vertical velocity: $V_{P0} = \sqrt{C_{33}/\rho}$;
- S-wave vertical velocity: $V_{S0} = \sqrt{C_{55}/\rho}$;
- $\epsilon = (C_{11} - C_{33})/2C_{33}$;
- $\delta = [(C_{13} + C_{55})^2 - (C_3 3 - C_{55})^2]/[2C_{33}(C_3 3 - C_{55})]$;
- $\gamma = (C_{66} - C_{55})/2C_{55}$.

We solve the full waveform inverse problem by minimizing an objective function $\mathcal{J}(\mathbf{u},\mathbf{m})$ consisting of a term that estimates the misfit between the predicted and observed data $\mathcal{J}_D(\mathbf{u},\mathbf{m})$ and a term that applies model constraints using a petrophysical penalty term, $\mathcal{J}_P(\mathbf{m})$, as proposed by Aragao and Sava (2020a).

Considering the vector of elastic model parameters $\mathbf{m}(\mathbf{x})$, we define $\mathcal{J}_P(\mathbf{m})$ based on the distances relative to all points of a multimodal PDF describing the petrophysical relations between the components of the anisotropic model parameters. This PDF is determined from well log data, for example, and represented by coordinates $\mathbf{p}$. For any given model represented by $\mathbf{m}$, we compute a distance to any point of the distribution by

$$d(\mathbf{m},\mathbf{p}) = \|\mathbf{m} - \mathbf{p}\|_2. \tag{2}$$

Then, using the probability density $f(\mathbf{p})$ described by the petrophysical PDF, we determine the distance $D(\mathbf{m})$ from $\mathbf{m}$ to the entire distribution as

$$\frac{1}{D(\mathbf{m})} = \sum_{\mathbf{p}} \frac{f(\mathbf{p})}{d(\mathbf{m},\mathbf{p})}. \tag{3}$$

Finally, the penalty term $\mathcal{J}_P$ is defined as

$$\mathcal{J}_P = a \sum_{\mathbf{m}} D(\mathbf{m}), \tag{4}$$

where the scalar parameter a determines the strength of the penalty term in the objective function.

Aragao and Sava (2020b) implement a modification to the technique proposed by Aragao and Sava (2020a) by considering

multiple PDFs in order to build $\mathcal{J}_P$, such that each PDF represents a different lithological unit. In this way, we refer to the objective function composed by the data misfit and the petrophysical probabilistic penalty term based on a single PDF as $\mathcal{J}_D + \mathcal{J}_{P1}$, and to the objective function composed by the data misfit and the petrophysical probabilistic penalty term based on multiple PDFs as $\mathcal{J}_D + \mathcal{J}_{P2}$.

3 EXAMPLES

We illustrate the technique with a portion of the Marmousi 2 model, where the available petrophysical information does not indicate the occurrence of separate lithological units. As proposed by Aragao and Sava (2020b), we use the K-means clustering technique to categorize the petrophysical information into multiple clusters, which represents different lithologies, in order to create different PDFs for the petrophysical penalty term. We compare inversions using only the data misfit term $\mathcal{J}_D$, with inversions combining data misfit with the petrophysical penalty based on a single PDF $\mathcal{J}_D + \mathcal{J}_{P1}$, or multiple PDFs $\mathcal{J}_D + \mathcal{J}_{P2}$.

We consider the anisotropic elastic model parameters as $\mathbf{m} = \{V_{P0}, V_{S0}, V_{P,hor}, V_{P,nmo}\}$, such that $V_{P,hor} = V_{P0}\sqrt{1+2\epsilon}$ and $V_{P,nmo} = V_{P0}\sqrt{1+2\delta}$. Then, in order to calculate the petrophysical penalty, one needs to evaluate distances to all points of a 4D PDF determined from the well log data, represented by coordinates $\mathbf{p} = \{V_{P0_p}, V_{S0_p}, V_{P,hor_p}, V_{P,nmo_p}\}$.

Figure 1 shows the correct V_{P0} V_{S0}, $V_{P,hor}$ and $V_{P,nmo}$ models and the well locations. We simulate a multicomponent survey with a line of receiver at $z = 0.05$ km and 50 evenly spaced sources located at $z = 0.025$ km. Figure 2 shows the initial model parameters.

Figure 3 shows the recovered models using the objective function $\mathcal{J}_D$. One can notice that all models have spurious artifacts due to interparameter crosstalk. Additionally, the model parameters have different resolutions due to the source-receiver geometry. As waves propagate predominantly close to the vertical direction, the inverted $V_{P,hor}$ model presents smaller resolution than the other parameters.

Figure 4 shows the recovered models using the objective function $\mathcal{J}_D + \mathcal{J}_{P1}$. The models are more blocky and conform better to the true models (Figure 1) than the models recovered using the $\mathcal{J}_D$ objective function (Figure 3). Moreover, all models depicted in Figure 4 have similar resolution.

Figure 5 shows the recovered models using the objective function $\mathcal{J}_D + \mathcal{J}_{P2}$. We use 4 clusters for the algorithm. The inverted models depicted in Figure 5 show high resolution and are closer to the true models (Figure 1) compared with the cases when we use the objective functions $\mathcal{J}_D$ (Figure 3) or $\mathcal{J}_D + \mathcal{J}_{P1}$ (Figure 4). Therefore, the subsurface structure and the magnitude of the model anomalies are better recovered when using an objective function that incorporates petrophysical information, and takes into account that the subsurface is composed of multiple lithologies.

Figures 6 and 7 show, respectively, the vertical and horizontal components of the residual constructed using, from the left to the right, the initial models, and the recovered models shown in Figures 3, 4 and 5. Note that the amplitudes of the data residuals obtained using the predicted data computed using the recovered models depicted in Figure 5 are much smaller compared to the case where the data are predicted using the models obtained for the unconstrained objective function $\mathcal{J}_D$ (Figure 3) or for the objective function $\mathcal{J}_D + \mathcal{J}_{P1}$ (Figure 4). Therefore, the multi-cluster petrophysical penalty term allows us to recover models that are more kinematically accurate then in the case of an objective function purely based on the data misfit $\mathcal{J}_D$ or an objective function that uses a petrophysical penalty based on a single PDF $\mathcal{J}_D + \mathcal{J}_{P1}$.

4 CONCLUSIONS

We incorporate petrophysical information into elastic full waveform inversion through a penalty term based on probability density functions (PDFs). We demonstrate that imposing this penalty improves the quality of the recovered anisotropic subsurface models and helps guide the results towards a more geologically plausible solution. Finally, we show that by using the penalty term based on multiple PDFs we can further enhance the resolution and accuracy of the anistropic model parameters, which helps predicting multicomponent data that match the observed data with accurate amplitude and phase.

5 ACKNOWLEDGEMENTS

We acknowledge CAPES (Brazilian Federal Agency for Support and Evaluation of Graduate Education) for financial support. We thank the sponsors of the Center for Wave Phenomena (CWP), whose support made this research possible. The synthetic examples in this paper uses the Madagascar open-source software package (Fomel et al., 2013) freely available from http://www.ahay.org.

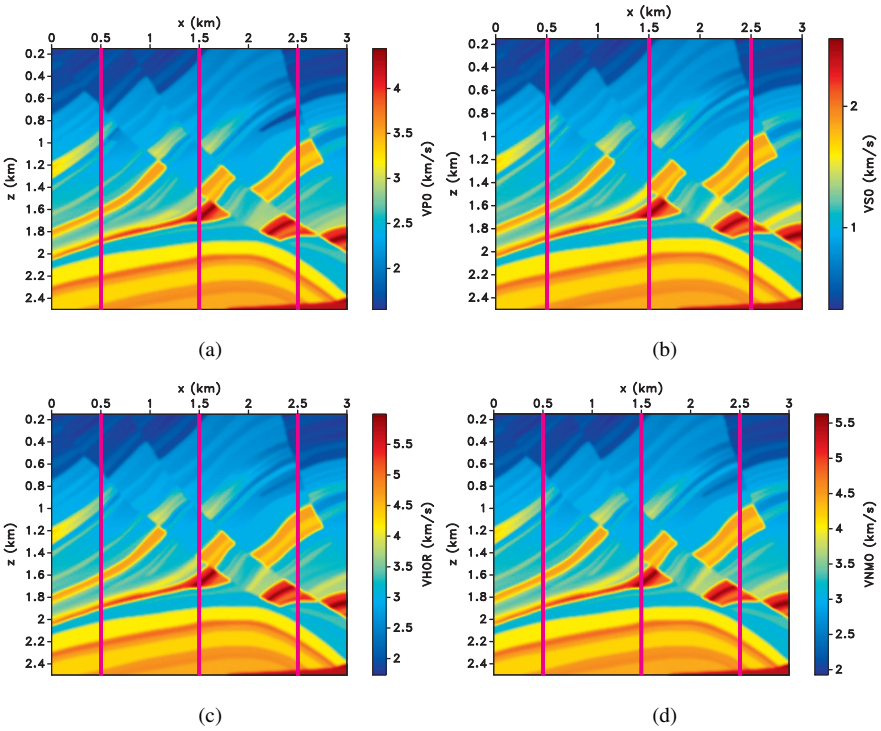


Figure 1. True (a) V_{P0}, (b) V_{S0}, (c) $V_{P,hor}$ and (d) $V_{P,nmo}$ models. The vertical lines correspond to well locations that provide information for the petrophysical penalty term.

REFERENCES

Aragao, O., and P. Sava, 2020a, Elastic full-waveform inversion probabilistic petrophysical model constraints: Geophysics, **85**, no. 2, R101–R111.

———, 2020b, Elastic full waveform inversion with probabilistic petrophysical clustering: Geophysical Prospecting, **68**, no. 4, 1341 – 1355.

Fomel, S., P. Sava, I. Vlad, Y. Liu, and V. Bashkardin, 2013, Madagascar: open-source software project for multidimensional data analysis and reproducible computational experiments: Journal of Open Research Software, **1**.

Operto, S., Y. Gholami, V. Prieux, A. Ribodetti, R. Brossier, L. Metivier, and J. Virieux, 2013, A guided tour of multiparameter full-waveform inversion with multicomponent data: from theory to practice: The Leading Edge, **32**, no. 9, 1040–1054.

Plessix, R. E., and Q. Cao, 2010, A parametrization study for surface seismic full waveform inversion in an acoustic vertical transversely isotropic medium: Geophysical Journal International, **185**, 539–556.

Pratt, R. G., Z. M. Williamson, and M. Warner, 1996, Two-dimensional velocity model from wide-angle seismic data by wavefield inversion: Geophysical Journal International, **124**, 323–340.

Tarantola, A., 1984, Inversion of seismic reflection data in the acoustic approximation: Geophysics, **49**, 1259–1266.

———, 1988, Theoretical background for the inversion of seismic waveforms including elasticity and attenuation: Pure and Applied Geophysics, **128**, 365–399.

Tsvankin, I., 2012, Seismic signatures and analysis of reflection data in anisotropic media: Society of Exploration Geophysics, Tulsa.

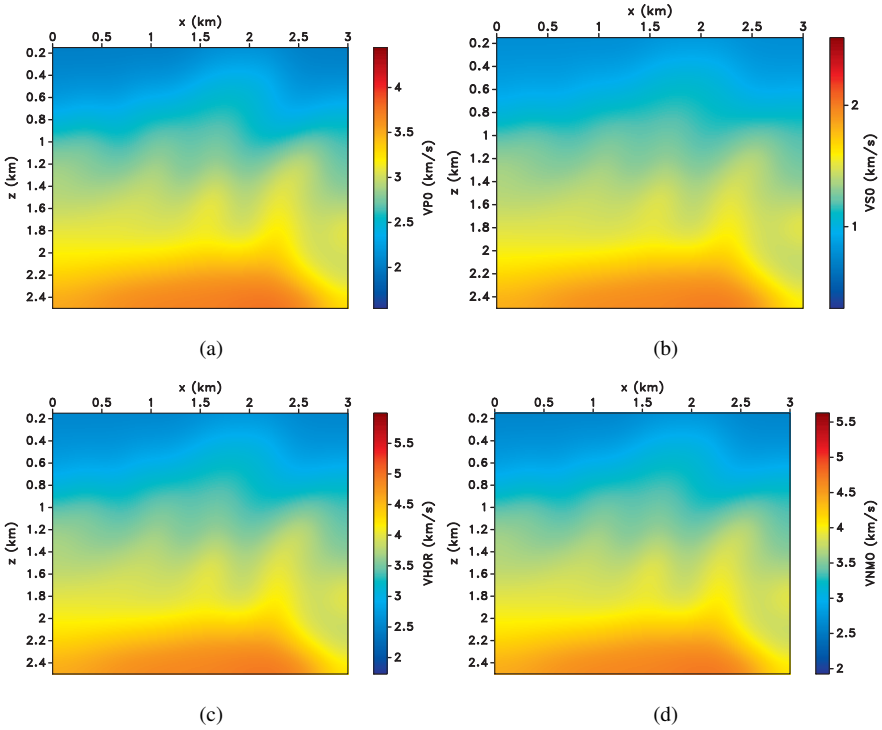


Figure 2. Initial (a) V_{P0}, (b) V_{S0}, (c) $V_{P,hor}$ and (d) $V_{P,nmo}$ models, which we obtain by smoothing the true models.

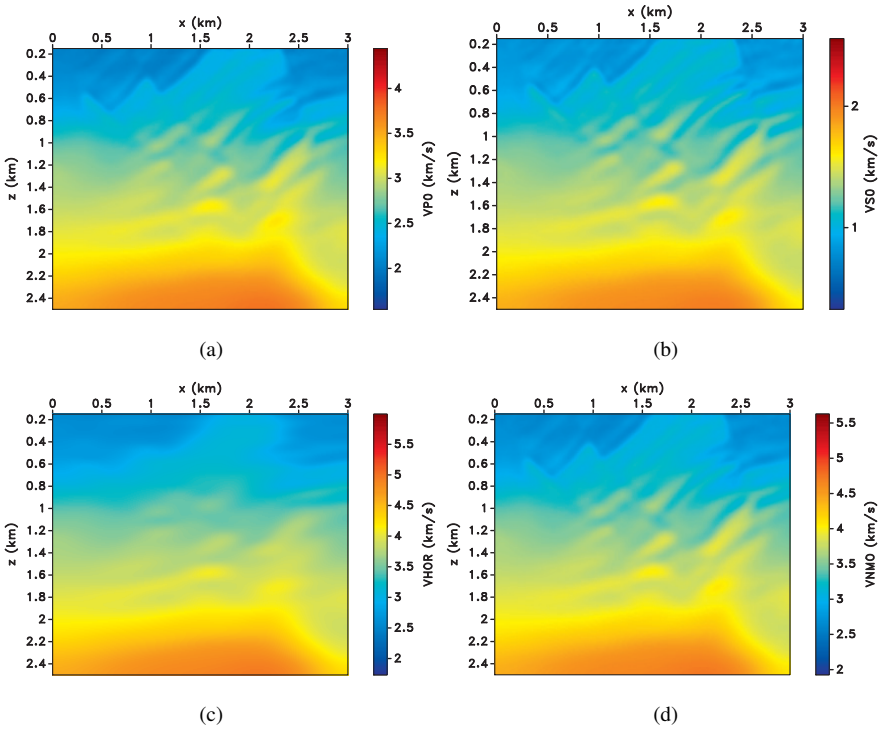


Figure 3. Recovered (a) V_{P0}, (b) V_{S0}, (c) $V_{P,hor}$ and (d) $V_{P,nmo}$ models using the objective function $\mathcal{J}_D$.

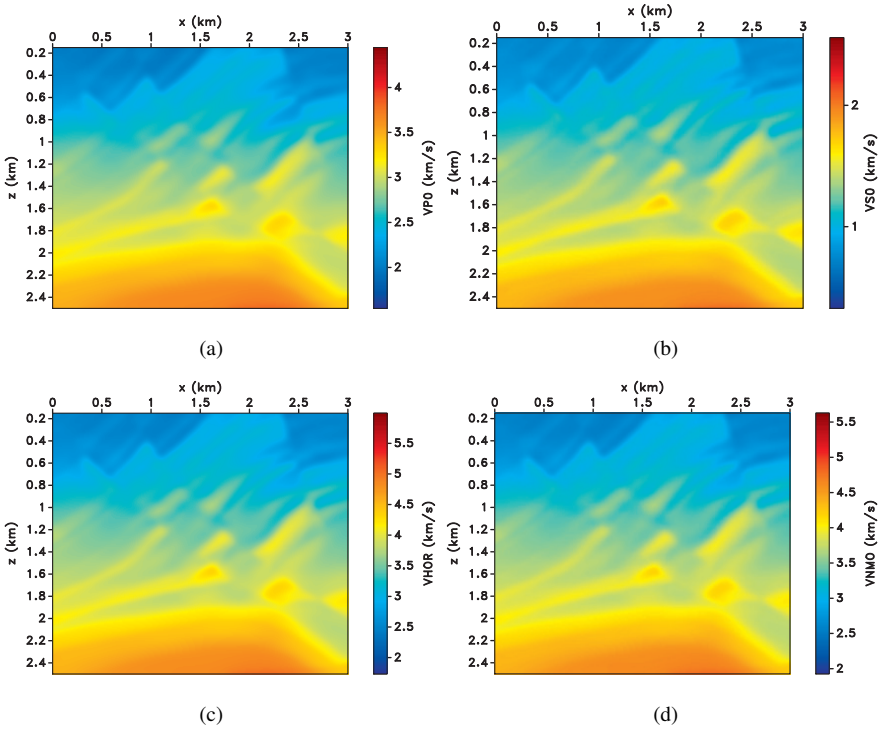


Figure 4. Recovered (a) V_{P0}, (b) V_{S0}, (c) $V_{P,hor}$ and (d) $V_{P,nmo}$ models using the objective function $\mathcal{J}_D + \mathcal{J}_{P1}$.

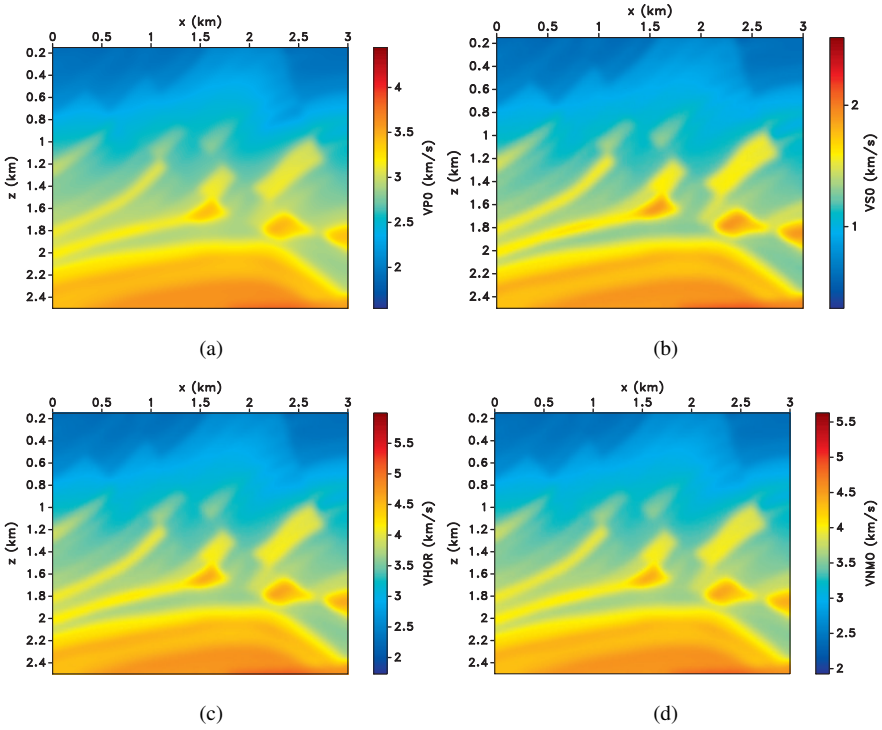


Figure 5. Recovered (a) V_{P0}, (b) V_{S0}, (c) $V_{P,hor}$ and (d) $V_{P,nmo}$ models using the objective function $\mathcal{J}_D + \mathcal{J}_{P2}$.

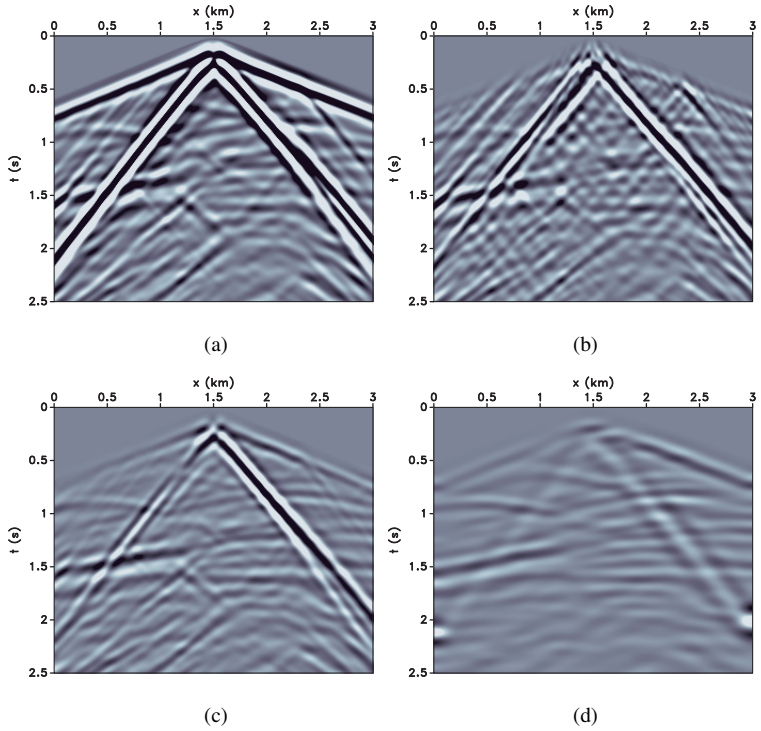


Figure 6. Vertical component of the data residuals using (a) the initial models (Figure 2), (b) the models recovered using the objective function $\mathcal{J}_D$ (Figure 3), or (c) $\mathcal{J}_D + \mathcal{J}_{P1}$ (Figure 4) or (d) $\mathcal{J}_D + \mathcal{J}_{P2}$ (Figure 5).

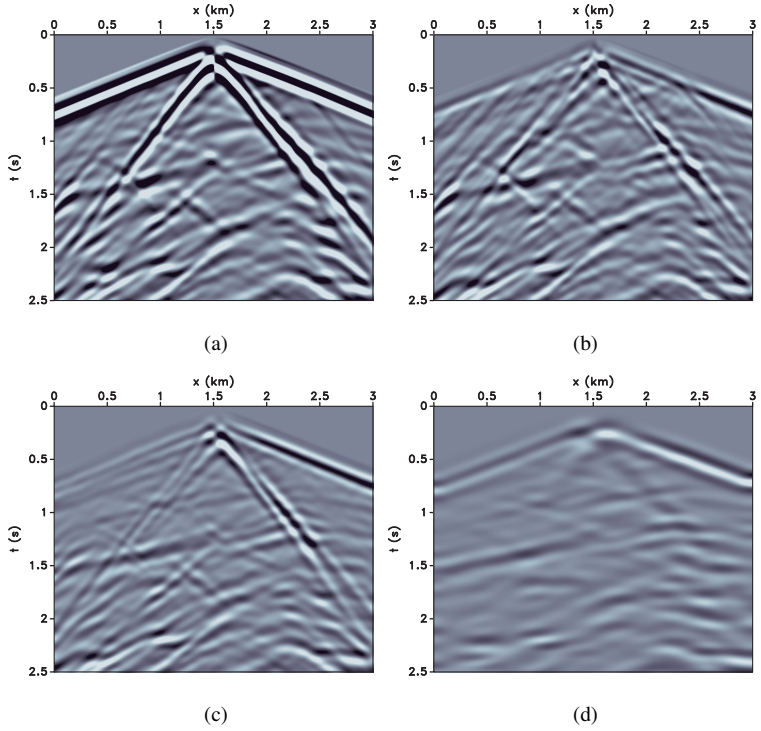


Figure 7. Horizontal component of the data residuals using (a) the initial models (Figure 2), (b) the models recovered using the objective function $\mathcal{J}_D$ (Figure 3), or (c) $\mathcal{J}_D + \mathcal{J}_{P1}$ (Figure 4) or (d) $\mathcal{J}_D + \mathcal{J}_{P2}$ (Figure 5).